Available online at www.sciencedirect.com
ScienceDirect
Journal of Molecular Catalysis A: Chemical 266 (2007) 118–130
JOURNAL OF MOLECULAR CATALYSIS A: CHEMICAL
www.elsevier.com/locate/molcata

Characterization and catalytic activity of cobalt containing MCM-41 prepared by direct hydrothermal, grafting and immobilization methods

Shrikant S. Bhoware, A.P. Singh *

Inorganic and Catalysis Division, National Chemical Laboratory, Pune 411 008, India

Received 14 August 2006; received in revised form 15 September 2006; accepted 18 September 2006
Available online 23 September 2006

Abstract

Cobalt containing hexagonal mesoporous molecular sieves (MCM-41) were prepared by different methods viz., direct hydrothermal synthesis, grafting and immobilization. The calcined material was characterized by various spectroscopic tools such as powder X-ray diffraction (XRD), N_2 adsorption–desorption isotherms, Fourier transformed infra-red (FT-IR) spectroscopy, scanning electron microscopy (SEM), transmission electron microscopy (TEM), diffuse reflectance UV–vis and X-ray photoelectron spectroscopy (XPS). The XRD patterns show the highly intense (100) reflection peak in the range 2–3° (2θ angle), characteristic of mesoporous material. Higher order reflection peaks suggest highly ordered mesoporous structure. N_2 adsorption–desorption isotherms are of type IV according to IUPAC classification and the steep rise in the isotherms in the narrow range 3.5–4.5 of relative pressure (P/P_0) is due to the condensation of N_2 gas molecules in the pores (characteristic of mesoporous structure). In FT-IR increase in the intensity of band at 960 cm^{-1} with the increase of the cobalt content in Co-MCM-41 samples indicate the incorporation of cobalt ions in the framework of MCM-41. SEM and TEM reveal spherical morphology for the cobalt substituted MCM-41. UV–vis spectra demonstrate the characteristic features of framework and extraframework cobalt in MCM-41. Cobalt is in +2 oxidation state as evidenced from UV–vis and XPS. The catalysts were tested for the side chain oxidation of ethylbenzene using 70 wt.% *tert*-butyl hydrogen peroxide as an oxidant with and without the use of solvent. Solvents have effect in the catalytic activity and selectivity. In the absence of solvent, substituted cobalt [Co-MCM-41 (50)] in the framework of MCM-41 gives maximum ethylbenzene conversion while higher selectivity to acetophenone was achieved over immobilized cobalt on the MCM-41. Leaching data shows, immobilized cobalt catalyst is well hetrogenized.

Keywords: Co-MCM-41; XRD pattern; Mesoporous; Isotherms; Ethylbenzene oxidation

1. Introduction

Ordered mesoporous molecular sieves, MCM-41 (discovered by Mobil in 1992), which have hexagonal arrangement of mono-dimensional pores with the pore diameter (20–100 Å) and large surface areas (more than 1000 $m^2\ g^{-1}$) are very attractive for the design of new selective heterogeneous catalyst in the production of fine chemicals on large scale [1–3]. One of the striking feature of this material is that the wide range of pore diameters can be obtained very easily by changing the alkyl chain length of the template molecule. Moreover, it has higher surface areas as well as high hydrocarbon sorption capacity [2]. Soon it was followed by invention of new materials like SBA-15, KIT-6 and HMS [4–6]. MCM-41 mesoporous materials have potential uses as catalyst and support materials for catalytically active metal and metal oxides. Metal containing MCM-41 has been studied as model catalyst for shape selective reactions of larger molecules, as a catalytic membrane, and for other important reactions such as reforming, oxidation and polymerization [7–10]. Because of the flexible structure of the amorphous silica wall, different kinds of heteroatom have been incorporated into the silica matrix with little structural deterioration. After the invention of mesoporous molecular sieves, efforts have been made in the area of incorporation of metal by different methods. Further investigation of different types of metal species and their effect in overall performance of the catalyst in the reaction of bulky molecules have been studied. The incorporation of cations like Al and Ti in the SiO_2 matrix results in a substantial increase of surface acidity as happens with the Zeolites and such solids can be employed as acid catalyst whereas incorporation of cations like Mn, Ni and Co lead to material with sites suitable for redox catalytic operations [11–15].

* Corresponding author. Tel.: +91 2590 2633; fax: +91 2590 2633.
E-mail address: ap.singh@ncl.res.in (A.P. Singh).

1381-1169/$ – see front matter © 2006 Elsevier B.V. All rights reserved.
doi:10.1016/j.molcata.2006.09.031

The commercial processes of selective side chain oxidation of alkyl aromatics are mainly based on homogeneous catalysis in solvents such as acetic acid and using oxygen as an oxidant [16–19]. The reaction temperature is about 160–180 °C and demands the use of autoclave reactors, which is made using the special and costly material due to the corrosive medium. Furthermore, the formation of brominated byproducts (when used bromine as an activator) is an issue. Therefore there is a need for the development of new heterogeneous catalytic process for the synthesis of aromatic aldehydes and ketones. Vanadium and molybdenum based catalysts have been widely studied for the side chain oxidation of alkyl aromatics [20–26]. Besides this iron based catalyst was studied for the selective oxidation of alkyl aromatics but the success is very limited [27,28]. Heterogenized Co bimetallic complexes anchored to silica have been shown to form peroxo complexes by exposure to oxygen atmosphere at room temperature and this peroxo compound has been shown to be an active species in cyclohexene oxidation at 170 °C [29]. It is also known that cobalt ion exchanged X and Y zeolites are active in the gas phase oxidation of benzyl alcohol [30]. Cobalt containing mesoporous molecular sieves have been achieved by different methods viz., one pot synthesis method, post synthesis and gas deposition [31–37]. It has been shown that catalytic activity is directly dependent on the isolated metal species.

The present work addressed the characterization and catalytic activity of cobalt containing MCM-41 materials prepared by various methods in the side chain oxidation of ethylbenzene.

2. Experimental

Chemicals used were fumed silica (99% SiO_2, Aldrich), cetyl trimethyl ammonium bromide (CTMABr, Aldrich), sodium hydroxide (NaOH, Merck), trimethoxy propyl amine silane [97% $(CH_3CH_2O)_3Si(CH_2)_3NH_2$] and cobalt acetylacetone [$Co(acac)_2$, 99%, across]. All the chemicals were used without further purification.

2.1. Synthesis

2.1.1. Synthesis of hexagonal mesoporous molecular sieves MCM-41

Fumed silica and cetyl trimethyl ammonium bromide were used as silica source and surfactant, respectively. In a typical synthesis, CTMABr was dissolved in sodium hydroxide (NaOH) solution. To this, fumed silica was added slowly and stirred for 6 h. The molar gel composition was as follows:

$1SiO_2$: 0.19CTMABr : 0.4NaOH : $78H_2O$

Finally pH of the gel was maintained at 10.9 using dil. HCl. The gel was transferred to glass bottle (autoclavable) and kept in oil bath maintained at 100 °C for 48 h. Mixture was filtered, washed several times with distilled water under vacuum and dried at 100 °C. The synthesized material was calcined at 525 °C for 12 h.

2.1.2. Synthesis of Co substituted MCM-41 (Co-MCM-41)

Co-MCM-41 was synthesized by direct hydrothermal method with different Si/Co ratio. Fumed silica was added slowly to the mixture of NaOH and CTMABr with constant stirring. After 1 h, calculated amount of cobalt acetylacetone for the respective Si/Co ratio was added and stirring was allowed for another 5 h.

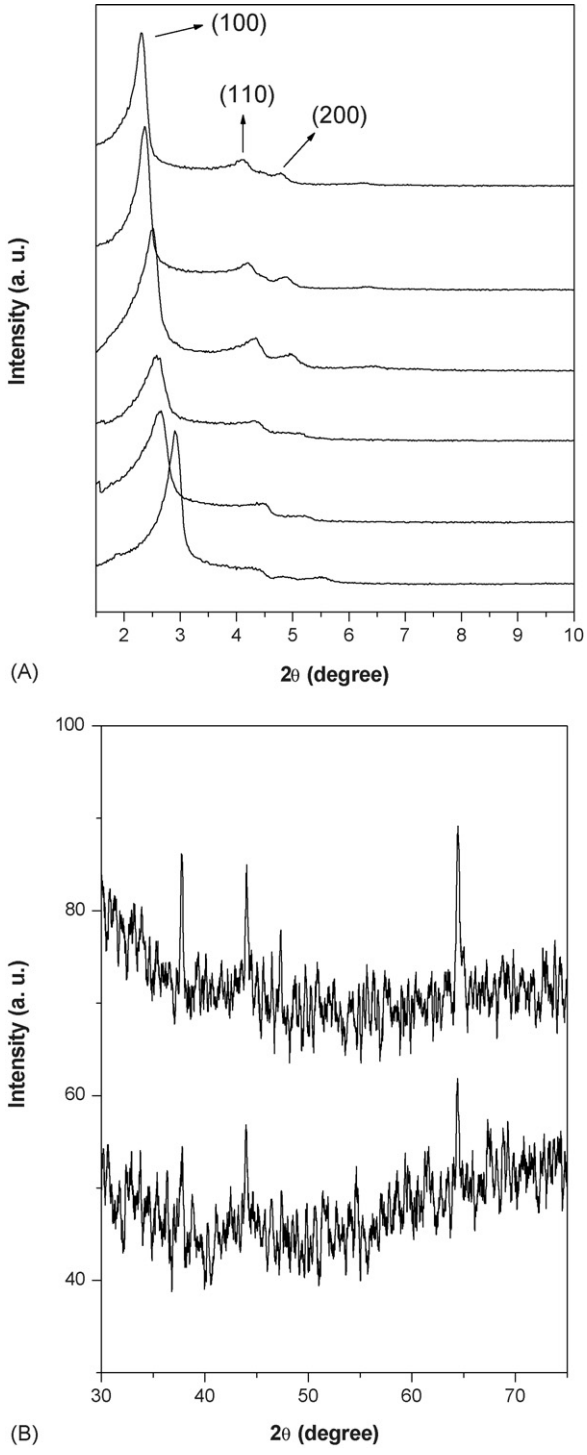

Fig. 1. XRD patterns of (A): (a) Co-MCM-41 (100), (b) Co-MCM-41 (50), (c) pure MCM-41, (d) Co/MCM-41 (1), (e) Co/MCM-41 (2) and (f) Co-/MCM-41; (B) higher angle XRD pattern for samples (a) and (b).

Table 1

Entry	Catalyst	Cobalt content (wt.%)[a]	2θ angle (degree)	a_0 (Å)[b]	S_{BET} ($m^2\ g^{-1}$)[c]	D_p (Å)[d]
1	MCM-41	–	2.50	40.80	1010	31.00
2	Co-MCM-41 (100)	0.92	2.31	44.11	1073	32.67
3	Co-MCM-41 (50)	2.10	2.37	43.00	1035	31.80
4	Co/MCM-41 (1)	0.81	2.56	39.82	832	29.91
5	Co/MCM-41 (2)	1.74	2.65	38.46	810	28.40
6	Co-/MCM-41	1.59	2.90	35.15	700	n.d.

n.d.: not determined.
[a] Cobalt content estimated by AAS analysis.
[b] Unit cell parameter values calculated using $a_0 = 2d_{100}/\sqrt{3}$.
[c] S_{BET} is the surface area calculated by BET method.
[d] D_p is the pore diameter.

The molar gel composition was:

$$1SiO_2 : x\,Co(acac)_2 :\ 0.19CTMABr :\ 0.4NaOH :\ 120H_2O$$

where 'x' is the calculated amount of cobalt acetylacetone for different Si/Co ratios. The pH of the gel was maintained at 10.5. The gel was transferred to autoclavable bottle kept in oil bath maintained at 100 °C for 3 days. Finally it was filtered, washed several times with distilled water and dried in air at 100 °C for 12 h. As synthesized material was calcined as described earlier. The materials were designated as Co-MCM-41 (100) and Co-MCM-41 (50) for Si/Co ratio of 100 and 50, respectively.

2.1.3. Synthesis of cobalt-grafted MCM-41 (Co/MCM-41)

Cobalt acetylacetone (0.094 and 0.182 g for 1 and 2 wt.% loading, respectively) was dissolved in anhydrous toluene. To this 2 g MCM-41 was added and refluxed at 100 °C for 12 h with constant stirring. Solvent was removed at its boiling temperatures using rotavapor. The sample was dried and calcined at 450 °C to remove the organic matter. They were designated as Co/MCM-41 (1) and Co/MCM-41 (2) for 1 and 2 wt.% cobalt loading, respectively.

2.1.4. Synthesis of cobalt immobilized on MCM-41 (Co-/MCM-41)

Equal moles of trimethoxy propyl amine silane and cobalt acetylacetone (0.175 g cobalt acetylacetone and 0.126 g trimethoxy propyl amine silane) were mixed in 100 ml toluene at room temperature for 6 h. After half an hour 2 g MCM-41 was added to the solution. The resulting solution was kept in oil bath maintained at 100 °C for 10 h with constant stirring. It was filtered, washed with acetone and dried at 70 °C for 6 h. Sample was designated as Co-/MCM-41.

2.2. Characterization

Powder X-ray diffraction pattern of the samples were recorded on a Rigaku D max III VC Ni filtered Cu Kα radiation, λ = 1.54 Å between 1 and 10 (2θ angle) with a scanning rate of 1 °C/min. The specific surface area, total pore volume and average pore diameter were measured by the N_2 adsorption–desorption method using NOVA 1200 (Quanta Chrome) instrument. The samples were activated at 300 °C for 3 h under vacuum and then adsorption–desorption was conducted by passing nitrogen over samples which was kept under liquid nitrogen. Pore size distribution was obtained by applying BJH pore analysis method to the desorption branch of nitrogen adsorption isotherm. SEM micrograph of the cobalt containing samples were obtained on JEOL-JSM 520 scanning microscope while the TEM images were performed on a JEOL-TEM 1200 EX instrument with 100 kV accelerating voltage to probe the mesoporosity of the material. Cobalt content in the samples was determined by atomic absorbance analysis using Perkin-Elmer 11013 spectrometer after dissolution of the samples in HCl–HF solution. Diffuse reflectance UV–vis spectra of the powder samples were recorded in the range 200–800 nm on Shimadzu UV 2101 PC spectrometer equipped with a diffuse reflectance attachment, using $BaSO_4$ as the reference. XPS measurements were performed on a VG Microtech ESCA 3000 instrument using non-monochromatized Mg Kα radiation at a pass energy of 50 eV and an electron take off angle of 60°. The correction of

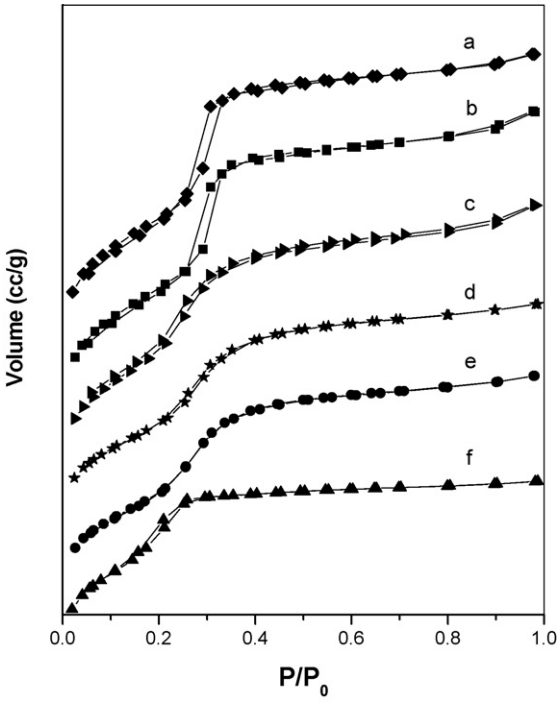

Fig. 2. N_2 adsorption–desorption isotherms of: (a) Co-MCM-41 (100), (b) Co-MCM-41 (50), (c) pure MCM-41, (d) Co/MCM-41 (1) (e) Co/MCM-41 (2) and (f) Co-/MCM-41.

binding energy (B.E.) was performed by using the C_{1s} peak of carbon at 285 eV as reference.

2.3. Catalytic reaction

Oxidation reactions of ethylbenzene (99% purity, Lancaster) were performed in a round bottom flask fitted with a water condenser using *tert*-butyl hydrogen peroxide (TBHP, 70 wt.%, Lancaster) as an oxidant. The reaction mixture of the ethylbenzene (1 g, 9.4 mmol) and TBHP (1.22 g, 9.4 mmol) was added to catalyst (5 wt.% with respect to ethylbenzene) and heated at constant temperature 80 °C under magnetic stirring. At different time interval, the reaction mixture was withdrawn by syringe. The products were analyzed by gas chromatograph (Agilent, HP 6890) equipped with a flame ionization detector (FID) and a capillary column (5 μm cross linked methyl silicone gum 0.2 mm × 50 m) and was further confirmed by GC-MS (Shimadzu 200A). Leaching of the metal during the course of reaction was verified by resubmission of the filtrate for further reaction at same reaction conditions.

3. Result and discussion

3.1. Powder X-ray diffraction

The XRD patterns of the calcined MCM-41, Co-MCM-41, Co/MCM-41 and Co-/MCM-41 are shown in Fig. 1A. MCM-41 mesoporous material exhibits four *hkl* diffraction peaks consistent with the highly ordered structure of a hexagonal pore arrays. The first diffraction peak in MCM-41 related to the (1 0 0) plane exhibits the highest intensity among all the calcined samples. In addition to main reflection peak at low angle (2θ), the less intense secondary reflections due to plane (1 0 0) (2 0 0) and (2 1 0) are well distinguished which indicate the higher long range ordering of the mesoporous channels [1,2]. In cobalt incorporated

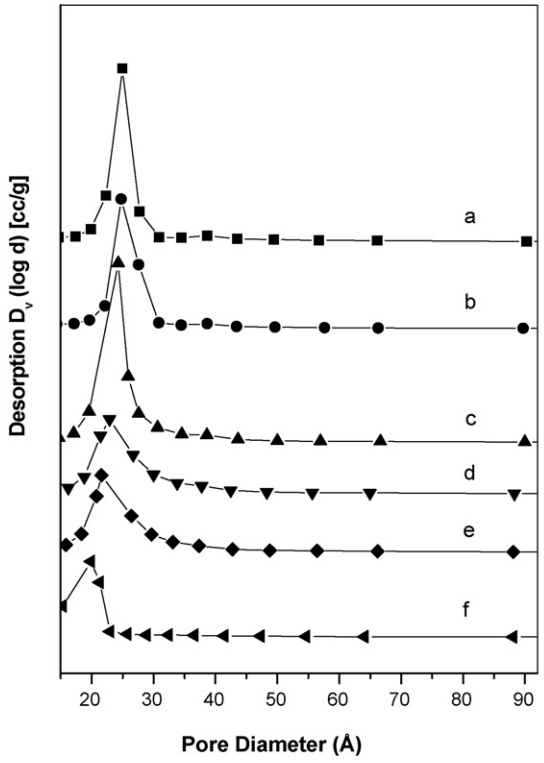

Fig. 3. Pore size distribution curves (calculated by BJH method) for the samples: (a) Co-MCM-41 (100), (b) Co-MCM-41 (50), (c) pure MCM-41, (d) Co/MCM-41 (1), (e) Co/MCM-41 (2) and (f) Co-/MCM-41.

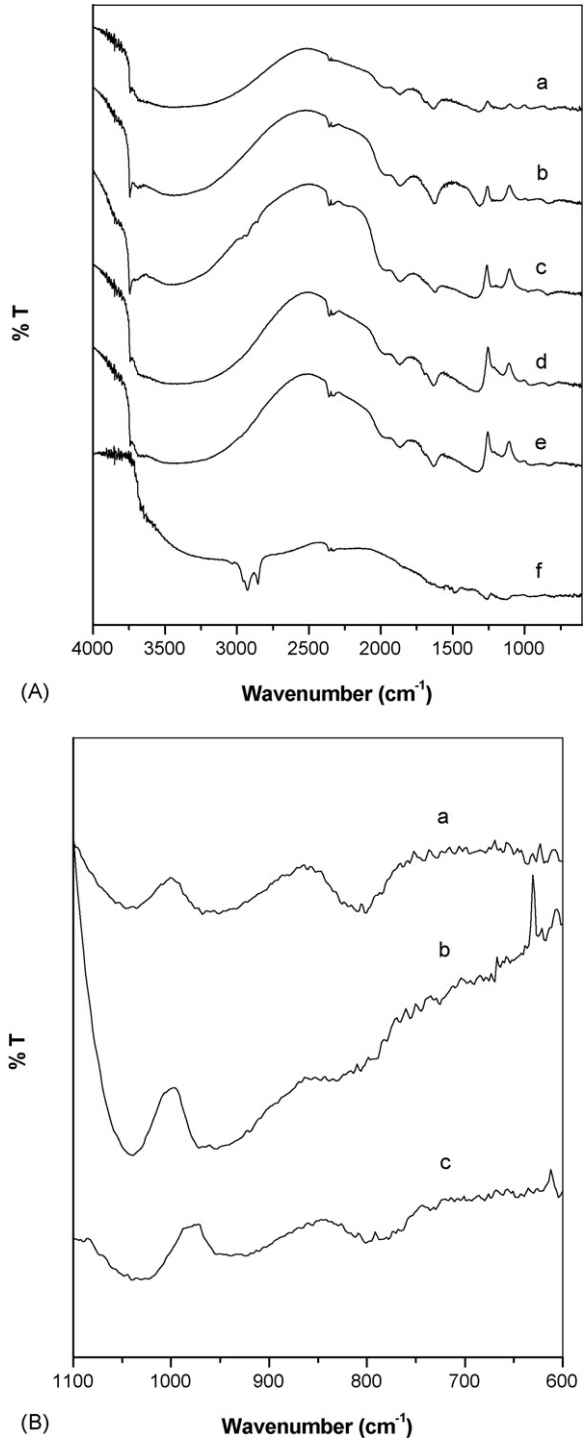

Fig. 4. FT-IR of (A): (a) Co-MCM-41 (100), (b) Co-MCM-41 (50), (c) pure MCM-41, (d) Co/MCM-41 (1), (e) Co/MCM-41 (2) and (f) Co-/MCM-41; (B) for samples (a), (b) and (c), it is shown in the range 1100–600 cm^{-1}.

MCM-41 (Si/Co = 100 and 50), four reflection peaks, characteristic of the hexagonal mesoporous structure, are clearly seen although the intensity is less when compared with pure MCM-41. It has been found that with the increase in cobalt content, intensity of the main peak (1 0 0) decreases. This indicates fall in long range ordering of the mesoporous channels after incorporating the cobalt ion. Lattice parameter value (a_0) was observed 40.8 Å for MCM-41. In Co-MCM-41 (100), a_0 value is 44.1 Å, which is more than the corresponding value for pure MCM-41. This shows the incorporation of cobalt in the framework. However, the decrease in the a_0 value has been observed for the sample Co-MCM-41 (50) but it is more than pure MCM-41 (Table 1). This is due to some cobalt ions settled on the mesoporous silica wall and slightly decreases the a_0 value when it is compared with Co-MCM-41 (100). Hence we conclude that only certain amount of cobalt is accommodated in the framework beyond which it prefers to settle on the silica framework. In the cobalt grafted MCM-41 samples, a_0 value decreases with the increasing amount of cobalt loading due to placement of the cobalt on the framework of MCM-41 thereby blocking the mesoporous channels. In cobalt immobilized MCM-41 samples, only (1 0 0) reflection peak is present. Absence of higher order reflection peaks indicate less ordering and homogeneity is lost after immobilization and hexagonal structure gets distorted. Moreover decrease in a_0 value is remarkable because of the presence of 3-amino propyl trimethoxy silane and cobalt. The higher angle XRD shows the presence of characteristic peaks of Co_3O_4 in cobalt incorporated MCM-41 (Fig. 1B). However the intensity is too low indicating the low amount of formation of microcrystal of cobalt oxide on the wall of MCM-41. It is very interesting to know that even for small amount of cobalt in Co-MCM-41 (100), peaks appeared in higher angle XRD. This may be due to synthesis procedure carried out in basic medium. Cobalt has property to form cluster like compound in highly basic condition.

3.2. N_2 adsorption–desorption isotherms

Nitrogen adsorption–desorption isotherms and the corresponding BJH pore size distribution were shown in Figs. 2 and 3 [38,39]. All the isotherms exhibit type IV isotherms (IUPAC

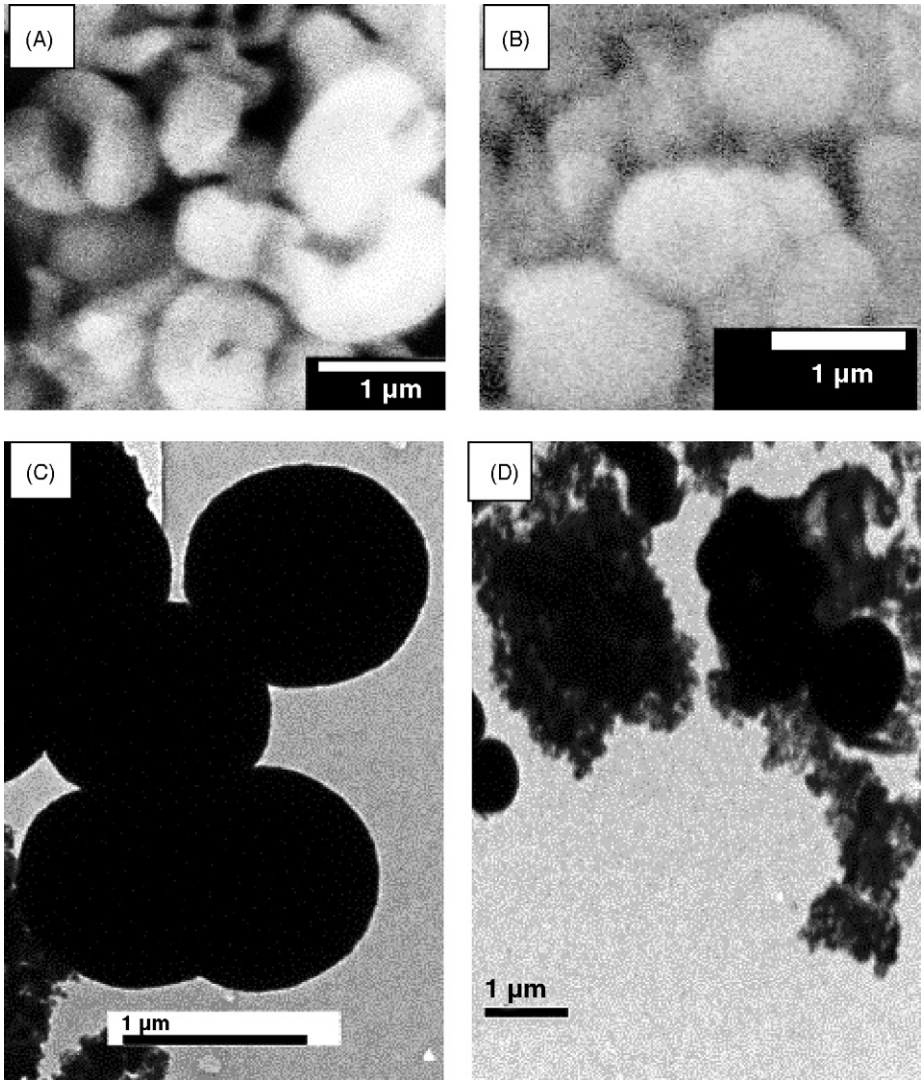

Fig. 5. SEM picture of: (A) pure MCM-41, (B) Co-MCM-41 (100); TEM picture of (C) pure MCM-41, (D) Co-MCM-41 (100).

classification), characteristic of mesoporous material, with a sharp inflection at a relative pressure (P/P_0) in the range 0.3–0.5 due to condensation of N_2 in the pore channels [1,2]. In the pore size distribution curve (Fig. 3), narrow and sharp peak is observed in the diameter range 20–25 Å showing uniform pore size. The isotherms of the cobalt incorporated samples (Co-MCM-41) show small hysterisis loop in the lower pressure regions. We noted that the surface area of Co-MCM-41 samples (1073 $m^2\,g^{-1}$) are comparatively more than pure MCM-41 (1010 $m^2\,g^{-1}$) and it is decreasing with the increase in metal content. The more surface for Co-MCM-41 is an indication of well dispersion of cobalt atoms. In grafted Co/MCM-41 (with cobalt loading 1 and 2 wt.%) and immobilized Co-/MCM-41samples surface area, pore volume and pore diameter was found decreased (Table 1). It is expected since in grafting and immobilization cobalt reside on the wall of mesoporous silica. It is found that for immobilized cobalt samples decrease in the surface area, pore volume and average pore diameter is more

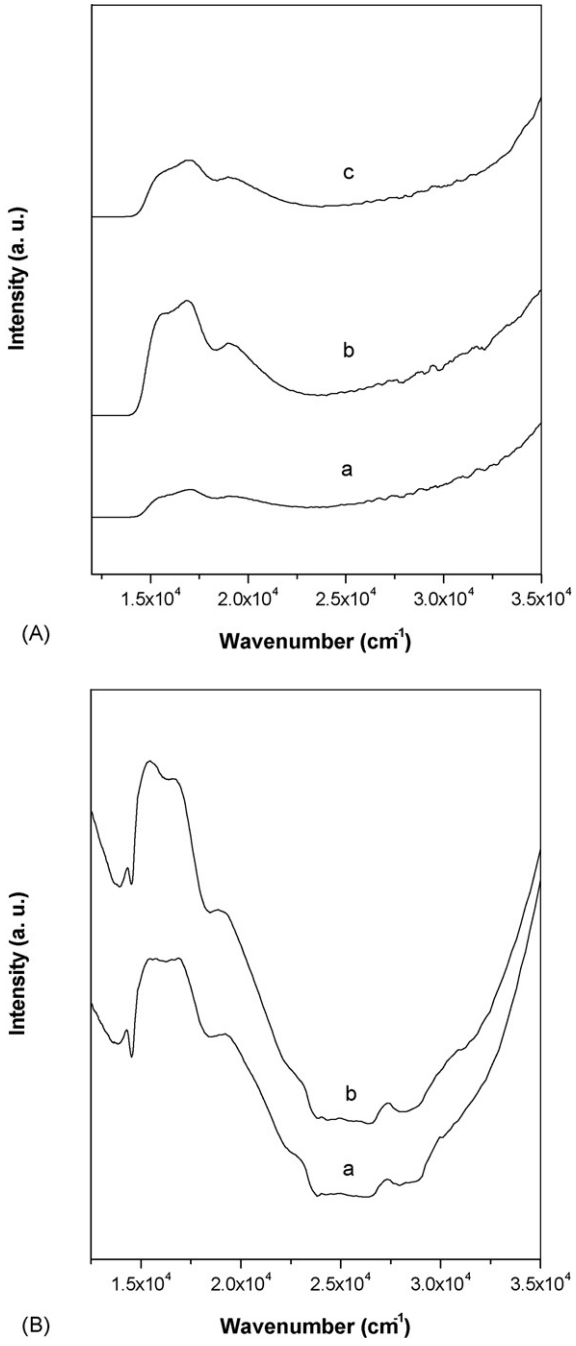

Fig. 6. UV–vis spectra of (A): (a) Co-MCM-41 (100), (b) Co-MCM-41 (50), (c) Co-/MCM-41; (B) (a) Co/MCM-41 (1), (b) Co/MCM-41 (2).

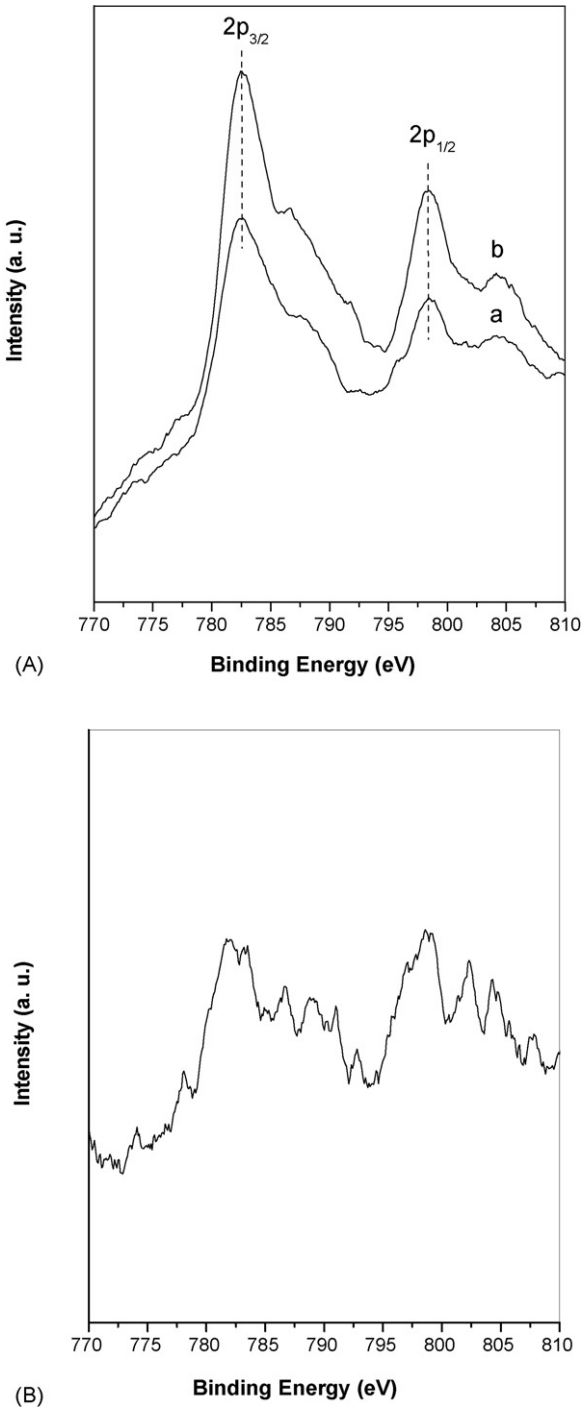

Fig. 7. XPS spectra of (A): (a) Co-MCM-41 (100) and (b) Co-MCM-41 (50); [B] Co/MCM-41 (2).

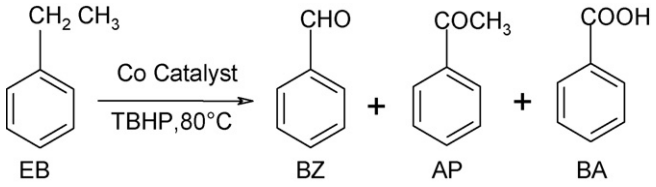

Scheme 1. Oxidation of ethylbenzene.

because of covalent bonding of the spacer on the wall of silica wall. This is in accordance with XRD result.

3.3. IR spectroscopy

Fig. 4A show the FT-IR spectra of the MCM-41 and cobalt containing MCM-41 in the range of 4000–400 cm^{-1}. Two bands around 1082 and 1228 cm^{-1} are associated to the internal and external asymmetric Si–O stretching modes. A strong band at 960 cm^{-1} is seen in the FT-IR spectra of MCM-41 and Co-MCM-41 which is attributed to stretching vibration of Si–O–Si and Si–O–Co bond. This band can be interpreted in terms of the overlapping of both Si–OH and Co–O–Si bond vibrations [40]. In Fig. 4B, it is clearly seen that the intensity of the peak at 960 cm^{-1} is increasing with the cobalt content, which is taken as the proof for the incorporation of cobalt ions. A sharp absorption band at 3738 cm^{-1} ascribed to free Si–OH groups. In the Co-/MCM-41 sample, the broad NH_2 stretching band at 3250–3450 cm^{-1} and N–H deformation peak at 1540–1560 cm^{-1} confirm the successful functionalisation of 3-amino propyl trimethoxy silane on the wall of MCM-41. It also displays the N–H bending mode (primary amine) at 1546 cm^{-1} and C–H stretching at 2944 cm^{-1}, which indicate the presence of $–Si(CH_2)_3NH_2$ on the wall surface [40].

3.4. Electron microscopy

Fig. 5 shows the SEM and TEM of MCM-41 and Co-MCM-41 (100). From the XRD results, it is clear that that morphology is hexagonal since high reflection peaks are present (characteristic of hexagonal structure). However the SEM and TEM show the morphology, which seems like spherical with uniform particle size. Earlier Haskouri et al. [33] reported the transformation of hexagonal to spherical morphology for the Co-MCM-41 material in spite of high reflection peaks in the XRD. TEM images clearly indicate that most of the particles are agglomerated in Co-MCM-41.

Table 2

Entry	Catalyst	Ethylbenzene conversion (wt.%)	Selectivity (wt.%)		
			BZ	AP	BA
1	MCM-41	–			
2	Co-MCM-41 (100)	36.1	18.2	71.0	9.5
3	Co-MCM-41 (50)	46.7	16.8	73.1	9.8
4	Co/MCM-41 (1)	25.0	20.3	65.1	14.5
5	Co/MCM-41 (2)	33.0	20.6	67.2	11.5
6	Co-/MCM-41	26.8	9.1	85.0	5.9

Reaction conditions: ethylbenzene 1 g; TBHP 1.22 g; catalyst 0.05 g; temperature 80 °C; reaction time 24 h (absence of solvent). BZ—benzaldehyde; AP—acetophenone; BA—benzoic acid.

3.5. UV–vis spectroscopy

Fig. 6 shows the DR UV–vis spectra of the calcined cobalt incorporated samples. All the samples exhibit triplet

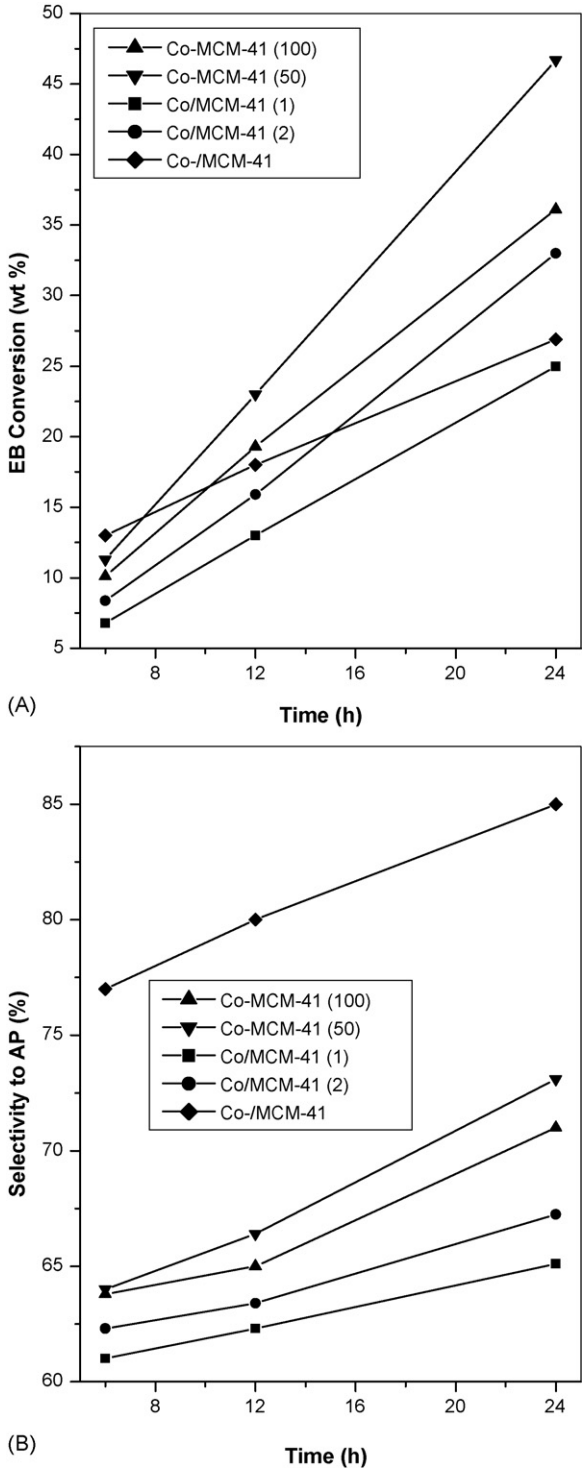

Fig. 8. Performance of various catalysts on: (A) ethylbenzene conversion vs. time and (B) selectivity to acetophenone vs. time.

absorption bands viz., 15,472, 17,015, and 19,019 cm^{-1} in the visible region. The triplet is assigned to $^4A_2(F) \rightarrow {}^4T_1(P)$ transition of Co(II) in the tetrahedral environment in the framework [36,41–43]. We observed that the intensity of the triplet is increasing with the metal content. Moreover the position of the peak at 17015 cm^{-1} is shifting towards the lower wavenumber which clearly shows the peak corresponding to framework tetrahedral Co(II) and extraframework tetrahedral Co(II) (which arises at 17,300 and 16,850 cm^{-1}) is overlapping [44]. After the triplet, shoulder appears in the energy range 19,500–22400 cm^{-1}. However, the intensity of this shoulder is more prominent in Co-MCM-41 with ratio Si/Co 50 than 100. This shoulder is due to octahedral Co(II) species and suggest that with increasing the cobalt content, octahedral species are increasing. Co/MCM-41 samples with different cobalt loading show characteristic transition corresponding to extraframework cobalt (II) in tetrahedral and octahedral coordination (Fig. 6B). All the synthesized cobalt containing samples were pink colored and after calcination color turns to deep blue (blue color is the characteristic of tetrahedral Co(II)) indicate the cobalt ions incorporated in the framework of mesoporous silica are in the divalent state with tetrahedral coordination geometry [45,46]. The spectra of the Co-/MCM-41 sample is same as Co-MCM-41 exhibiting triplet absorption bands at 15,472, 17,015, and 19,019 cm^{-1} in the visible region.

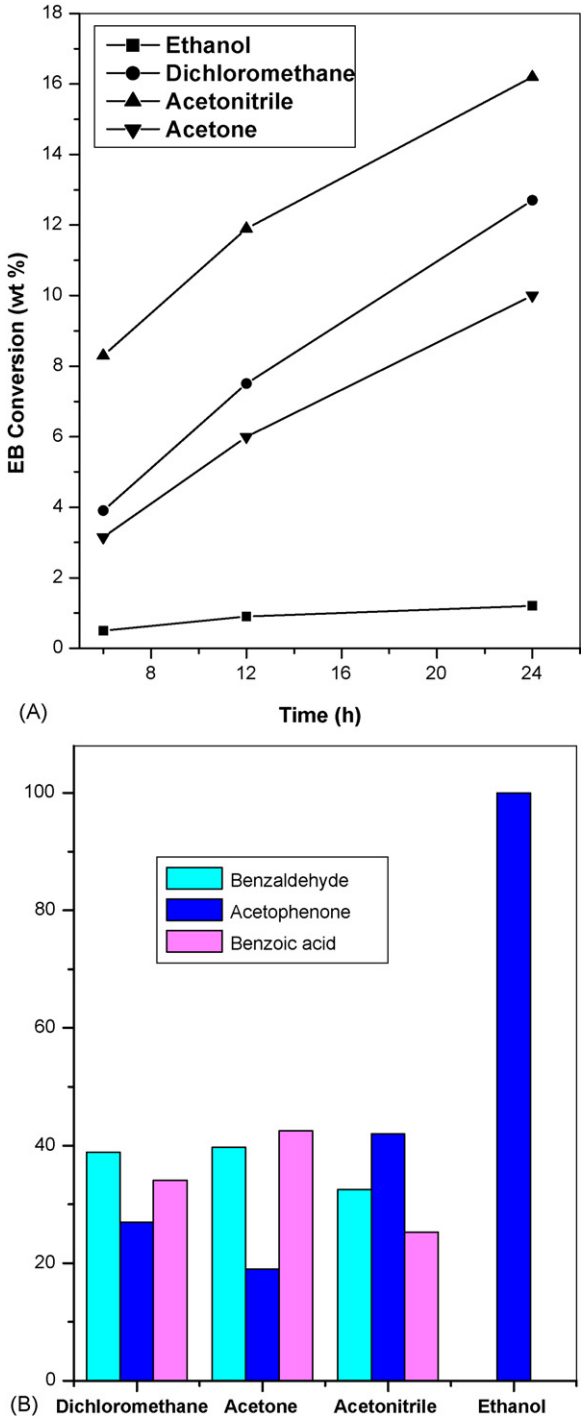

Fig. 9. Effect of various solvents on: (A) ethylbenzene conversion vs. time and (B) selectivity (after 24 h) over Co-MCM-41 (100).

3.6. X-ray photoelectron spectroscopy

Fig. 7A illustrates the X-ray photoelectron spectra of Co-MCM-41 samples with Si/Co ratio 100 and 50. The Co2p transition splits into two peaks, $2p_{3/2}$ and $2p_{1/2}$. For the isolated cobalt binding energy value occurs at 782.2 and 797 eV for the $2p_{3/2}$ and $2p_{1/2}$, respectively. We observed that intensities of $2p_{3/2}$ and $2p_{1/2}$ peaks are increased with increasing the cobalt content. In these samples $2p_{3/2}$ peak was found at the energy value 782.4 eV suggesting the strong interaction of tetrahedral Co(II) with the silica wall [47]. It is important to note that the relative intensity of the shake up satellite slightly increases with

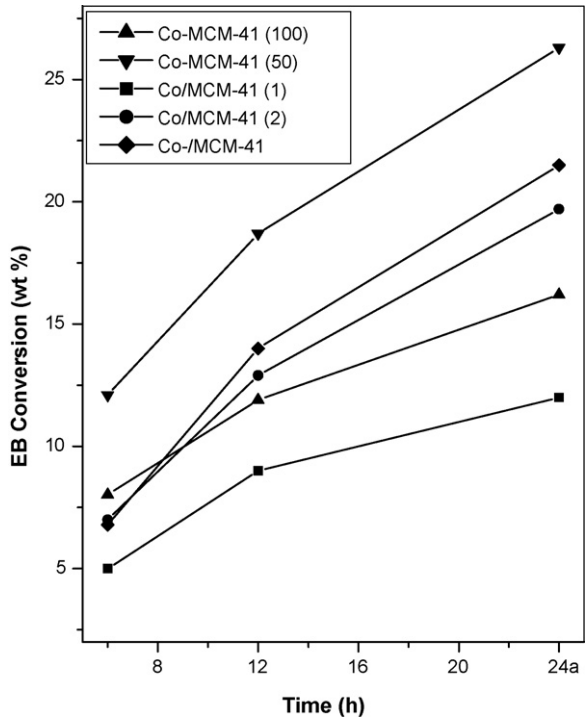

Fig. 10. Performance of the various catalysts in presence of acetonitrile with time.

respect to the increasing cobalt content and this feature is indicative of the presence of Co(II) species in the octahedral symmetry as found in CoO [48]. In cobalt grafted samples (Fig. 7B), Co/MCM-41 (2), the position of the $2p_{3/2}$ and $2p_{1/2}$ peaks are not been well identified but they were observed in Co–HMS (2). The higher surface area of MCM-41 (1010 $m^2\,g^{-1}$; for HMS it is 503 $m^2\,g^{-1}$) may play role in preventing the formation of bulk cobalt species [37(a)].

4. Catalytic performance

The oxidation of ethylbenzene was carried out in liquid phase results in the formation of the three main important products viz., benzaldehyde (BZ), acetophenone (AP) and benzoic acid (BA) (Scheme 1). BA is formed by over oxidation of BZ in the consecutive reaction steps. The EB oxidation was carried out using different oxidants such as hydrogen peroxide (H_2O_2)

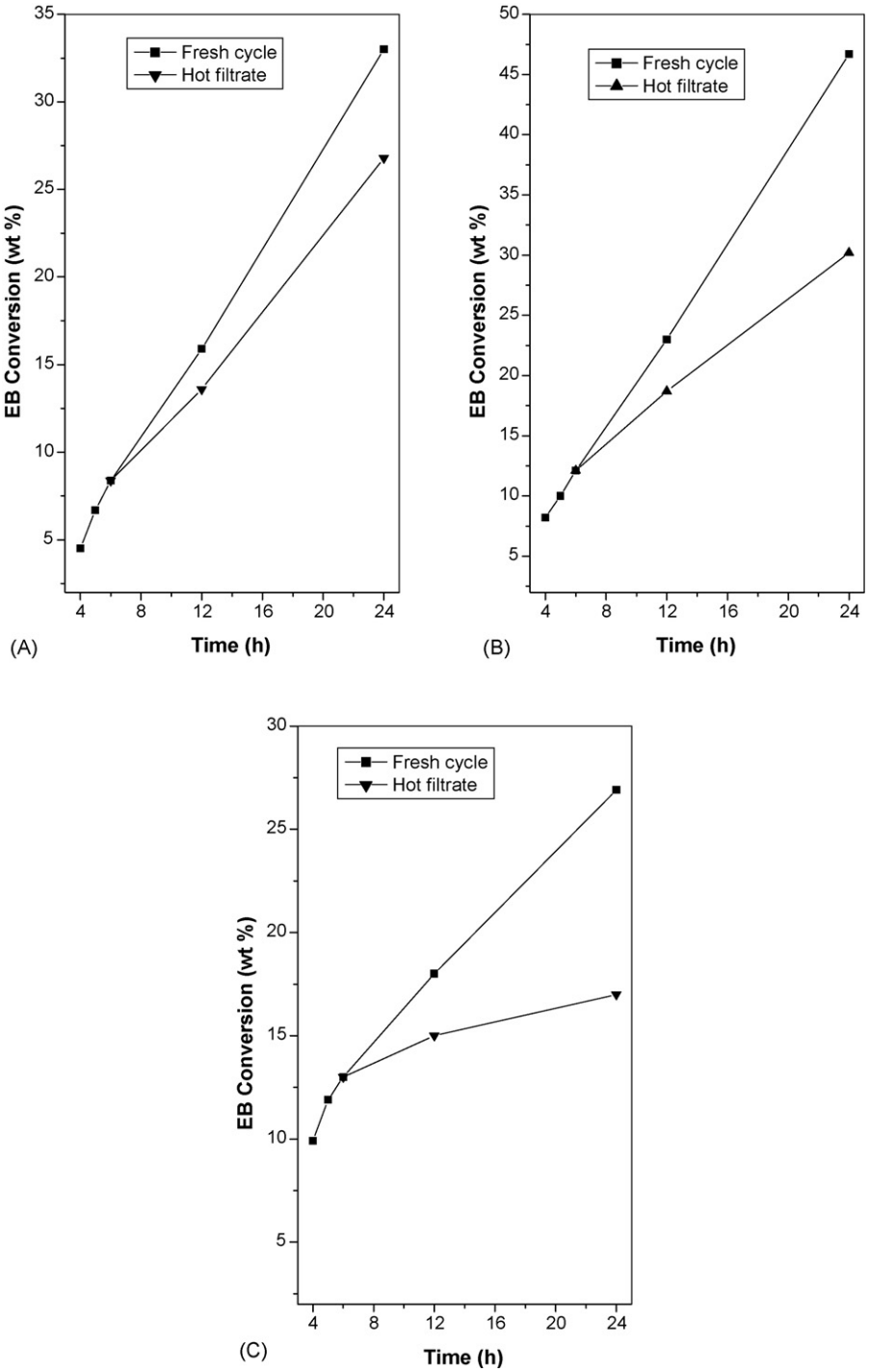

Fig. 11. Leaching study over different catalysts in absence of solvent: (A) Co/MCM-41 (2), (B) Co-MCM-41 (50) and Co-/MCM-41 (for leaching study, catalyst was removed after 6 h and filtrate was used for the further reaction).

[30 wt.%], *tert*-butyl hydrogen peroxide (TBHP) [70 wt.%] and sodium hypochlorite (NaOCl) [4 wt.%]. When NaOCl and H_2O_2 used as oxidant the activity for the EB oxidation was negligible.

Remarkable activity was found when TBHP was used as an oxidant. In order to check the effect of substrate to oxidant ratio on the catalytic performance, the reactions were studied at ratio of EB:TBHP (1:1, 1:2 and 1:3). It was observed that catalytic activity is not affected by different ratio of EB:TBHP. This result is opposite as observed by Singh et al. [49] with Co–APO-11 where EB conversion and selectivity to AP were affected by different amount of TBHP.

We noted that all the cobalt containing catalysts perform excellently in absence of solvent for the oxidation of EB. When different solvents were used, EB conversion was found lower than in the absence of solvent. This indicates that there is competition between the EB and solvent molecules for the active cobalt sites. With all the cobalt containing catalysts, conversion increases with reaction time. It was observed that EB conversion

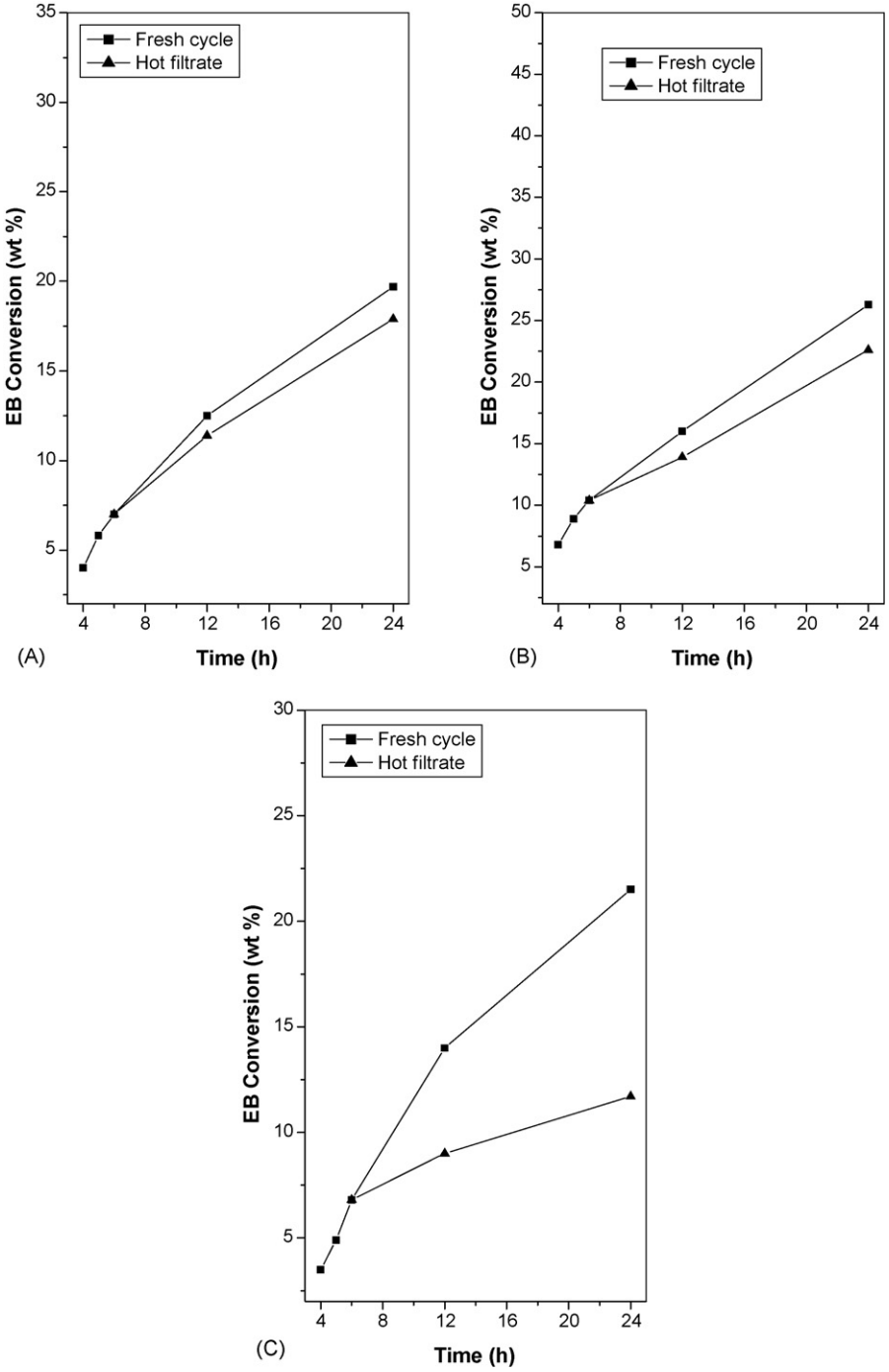

Fig. 12. Leaching study over different catalysts in presence of acetonitrile: (A) Co/MCM-41 (2), (B) Co-MCM-41 (50) and Co-/MCM-41 (for leaching study, catalyst was removed after 6 h and filtrate was used for the further reaction).

is found higher over incorporated cobalt catalyst than grafted and immobilized cobalt (Table 2). Moreover, it is observed that with Co-MCM-41 samples, EB conversion increases with the increase in the amount of cobalt. For Co-MCM-41 (100) and Co-MCM-41 (50), the EB conversion in absence of solvent after 24 h were found 36.1 and 46.7%, respectively (Fig. 8A). The selectivity to AP was increased slightly after 24 h in absence of solvent (71 and 73% for Co-MCM-41 (100) and Co-MCM-41 (50), respectively (Fig. 8B)). Some extraframework octahedral cobalt species were found in Co-MCM-41 (50) as evidenced from UV–vis spectra. The catalytic results indicate that, the extra framework cobalt species also contribute to the EB conversion. Co/MCM-41 (1) and Co/MCM-41 (2) catalysts in the absence of solvent after 24 h gives 25 and 33% EB conversion, respectively, which is lower than cobalt substituted MCM-41 catalyst. Even the selectivity to AP (65.1 and 67.2% for Co/MCM-41 (1) and Co/MCM-41 (2) after 24 h, respectively) is lower than observed with cobalt substituted MCM-41 catalyst (Table 2). For Co-/MCM-41, though the EB conversion (26.8%) is less, the highest selectivity to AP (85%) was achieved among all the cobalt containing MCM-41 catalyst under study. When the cobalt species were immobilized on the solid support through the spacer, their points of attachment are removed from one another. Thus these active species are so far apart that the resulting solid can be seen as single site catalyst [50]. Another reason for the high selectivity to AP may be from the bond formed between cobalt and nitrogen (of the spacer) which makes the cobalt less hungry (because of donation of lone pair of electron from nitrogen to vacant d orbital). This may effect in reacting or coordinating cobalt with the ethylbenzene in selective manner.

Solvent effect is apparent when the reaction was studied in different solvents like ethanol, dichloromethane, acetone and acetonitrile. In different solvents, EB conversion after 24 h over Co-MCM-41 (100) is in the order of acetonitrile > dichloromethane > acetone > ethanol (Fig. 9A). Selectivity to AP in different solvents follows the order ethanol > acetonitrile > dichloromethane > acetone (Fig. 9B). When acetone was used as solvent, the reaction follows the pathway more selectively to BZ and BA. In acetone, AP is converting to BZ by overoxidation of methyl group of AP followed by release of CO_2 [51]. This fact indicates that rate of side reaction becomes faster with the progress of the reaction leading to increase in the selectivity to BZ and BA.

The catalytic activity of Co-MCM-41 (100), Co-MCM-41 (50), Co/MCM-41 (1), Co/MCM-41 (2) and Co-/MCM-41 were studied in acetonitrile medium. The rate of EB conversion after 24 h over different catalyst follows the order Co-MCM-41 (50) > Co-/MCM-41 > Co/MCM-41 (2) > Co-MCM-41 (100) > Co/MCM-41 (1) (Fig. 10). Unlike in the absence of solvent, the selectivity to AP decreased with the progress of reaction. This indicate that rate of side reaction becomes more prominent with the progress of the reaction leading to increase in the selectivity to BZ and BA.

In order to find the heterogeneity of the catalyst, leaching study was carried out using hot filtrate (catalyst was removed after 6 h) at similar reaction conditions. From Figs. 11 and 12, it is clear that catalysts are prone to leaching. However, the Co-/MCM-41 shows less leaching (Figs. 11(C) and 12(C)) compared with Co/MCM-41 (2) and Co-MCM-41 (50). This can be explained in terms of the dative bond (which is strong) formed between the cobalt and nitrogen (of the spacer) in the immobilized sample. It was observed that the leaching in the ethylbenzene oxidation reaction, when carried out in the solvent (acetonitrile) medium, is more than in the absence of the solvent. This indicate that cobalt species have more affinity for the solvent molecules. Thus it is concluded that cobalt is well heterogenized in the immobilized sample than in incorporated and grafted samples.

Finally taking into account all the above reaction results, the probable mechanism is shown in Scheme 2. The oxidation of the ethylbenzene with TBHP is supposed to occur by free radical mechanism, yielding primarily ethylbenzenehydroperoxide [52,53]. The reaction may proceed by two ways (paths A and B). Since the secondary radical is more stable than primary radical, path A is more favorable. In the reaction mixture, no products (2-phenyl acetaldehyde and 2-phenyl acetic acid) were

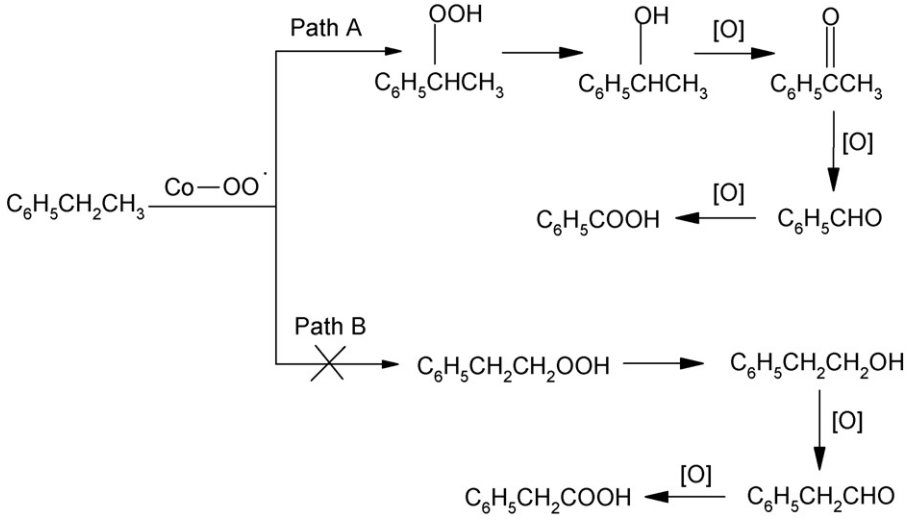

Scheme 2. Mechanistic pathway for the formation of different products in the oxidation of ethylbenzene.

detected from path B. BZ and BA are forming as overoxidized products of AP.

5. Conclusion

Cobalt containing MCM-41 catalysts were synthesized by direct hydrothermal synthesis, post synthesis and immobilization methods. Increase in the value of lattice expansion parameter in Co-MCM-41 samples reveals the incorporation of cobalt in the framework of MCM-41. In Co-MCM-41 sample, surface area was found higher than MCM-41 indicating well dispersion of cobalt ions. However, it is decreasing with the metal content in the grafted samples. In FT-IR, increase in the intensity of the peak at 960 cm^{-1} indicates the incorporation of the cobalt ion in the framework. TEM and SEM images show the spherical (considered as distorted hexagonal) morphology for the Co-MCM-41 sample. As the cobalt content increase, octahedral Co^{2+} is predominant species and reside on the surface of the wall as is evidenced from the UV–vis spectra. XPS shows the binding energy value corresponds to cobalt in +2 oxidation state. In the absence of solvent the conversion of ethylbenzene was found maximum with TBHP as an oxidation with remarkable increase in selectivity to acetophenone. Among the different solvent, catalytic activity is found more in acetonitrile. Immobilized catalyst was found highly selective to acetophenone in the oxidation of ethylbenzene in the absence of solvent using TBHP as an oxidant. From leaching study, it is clear that immobilized cobalt catalyst is resistant to leaching than incorporated and grafted cobalt catalyst.

Acknowledgement

SSB thanks Council of Scientific and Industrial Research (CSIR), New Delhi for awarding research fellowship.

References

[1] C.T. Kresge, M.E. Leonowicz, W.J. Roth, J.C. Vartuli, J.S. Beck, Nature 359 (1992) 710.
[2] J.S. Beck, J.C. Vartuli, W.J. Roth, M.E. Leonowicz, C.T. Kresge, K.D. Schmitt, C. Chu, D.H. Olson, E.W. Sheppard, S.B. McCullen, J.B. Higgins, J.L. Schenkler, J. Am. Chem. Soc. 114 (1992) 10834.
[3] P. Venuto, Stud. Surf. Sci. Catal. 105 (1997) 811.
[4] Q. Huo, R. Leon, P.M. Petroff, G.D. Stucky, Science 268 (1995) 1324.
[5] R. Ryoo, J.M. Kim, J.Y. Lee, C.H. Shin, Proceedings of the 11th International Zeolite Conference, Seoul, 1996.
[6] P.T. Tanev, M. Chibwe, T.J. Pinnavaia, Nature 368 (1994) 321.
[7] M. Guisnet, N.S. Gnep, S. Morin, J. Patarin, F. Loggia, V. Solinas, Mesoporous Molecular Sieves 117 (1998) 591.
[8] S. Morin, P. Ayrault, S. ElMouahid, N.S. Gnep, M. Guisnet, Appl. Catal. A 159 (1997) 317.
[9] C. Constantin, V. Parvulescu, A. Bujor, G. Popescu, B.L. Su, J. Mol. Catal. A 208 (2004) 245.
[10] V. Parvulescu, C. Constantin, G. Popescu, B.L. Su, J. Mol. Catal. A 208 (2004) 253.
[11] J.M. Campelo, D. Luna, R. Luque, J.M. Marinas, A.A. Romero, J.J. Calvino, M.P. Rodrýguez-Luque, J. Catal. 230 (2005) 327.
[12] D. Zhao, C. Nie, Y. Zhou, S. Xia, L. Huang, Q. Li, Catal. Today 68 (2001) 11.
[13] M.L. Occelli, S. Biz, A. Auroux, Appl. Catal. A 183 (1999) 231.
[14] R.M. Barrer, Hydrothermal Chemistry of Zeolites, Academic Press, New York, 1982.
[15] V.N. Romannikov, V.M. Mastikhin, S. Hocevar, B. Drzaj, Zeolites 3 (1983) 311.
[16] G. Centi, F. Cavani, F. Trifiro, M.V. Twigg, M.S. Spencer (Eds.), Selective Oxidation by Heterogeneous Catalysis: Recent Developments, Fundamental and Applied Catalysis, Kluwer/Plenum Publishing Corporation, New York and London, 2001.
[17] P. Arpentinier, F. Cavani, F. Trifiro, The Technology of Catalytic Oxidations. 1. Chemical Catalytic and Engineering Aspects, Editions TECHNIP, Paris, France, 2001.
[18] G. Centi, S. Perathoner, Selective oxidation, Section E, Industrial Processes and Relevant Engineering Issues, in: I.T. Horva'th (Ed.), Encyclopedia of Catalysis, Wiley, New York, 2003.
[19] E.O. Ohsol, Hydrocarbon oxidation, in: J.J. McKetta (Ed.), Encyclopedia of Chemical Processing and Design, vol. 33, Marcel Dekker, New York, 1987, pp. 36–45.
[20] A. Bruckner, U. Bentrup, A. Martin, J. Radnik, L. Wilde, G.-U. Wolf, Stud. Surf. Sci. Catal. A 130 (2000) 359.
[21] D.A. Bulushev, L. Kiwi-Minsker, V.I. Zaikovskii, A. Renken, J. Catal. 193 (2000) 145.
[22] F. Konietzni, H.W. Zanthoff, W.F. Maier, J. Catal. 188 (1999) 154.
[23] S.D. Val, M.L. Granados, J.L.G. Fierro, J. Santamaria-Gonzalez, A. Jimenez-Lopez, J. Catal. 188 (1999) 203.
[24] J.S. Yoo, J.A. Donohue, M.S. Kleefish, P.S. Lin, S.D. Elfine, Appl. Catal. A 105 (1993) 83.
[25] J.S. Yoo, C. Choi-Feng, J.A. Donohue, Appl. Catal. A 118 (1994) 87.
[26] J.S. Yoo, Appl. Catal. A Gen. 143 (1996) 29.
[27] G. Centi, S. Perathoner, S. Tonini, Topics Catal. 11 (2000) 195.
[28] G. Centi, S. Perathoner, S. Tonini, Catal. Today 61 (2000) 211.
[29] E. Solomon, F. Tuczek, D.E. Root, C.A. Brown, Chem. Rev. 94 (1994) 827.
[30] T. Seiki, A. Nakato, S. Nishiyama, S. Tsuruya, Phys. Chem. Chem. Phys. 5 (2003) 3818.
[31] T. Vraćlstad, G. Øye, M. Rønning, W.R. Glomm, M. Stocker, J. Sjoblom, Micropor. Mesopor. Mater. 80 (2005) 291.
[32] S. Lim, D. Ciuparu, C. Pak, F. Dobek, Y. Chen, D. Harding, L.P. Ferle, G. Haller, J. Phys. Chem. B 107 (2003) 11048.
[33] J. El Haskouri, S. Cabrera, C.J. Gomez-Garcia, C. Guillem, J. Latorre, A. Beltran, D. Beltran, M.D. Marcos, P. Amoros, Chem. Mater. 16 (2004) 2805.
[34] A.D. Badiei, L. Bonneviot, Inorg. Chem. 37 (1998) 4142.
[35] A. Tuel, in: L. Bonneviot, F. Beland, C. Danumah, S. Giasson, S. Kaliaguine (Eds.), Proceedings of the 1st International Symposium on Mesoporous Molecular Sieves, vol. 117, Stud. Surf. Sci. Catal, Elsevier, Amsterdam, 1998.
[36] A. Vinu, J. Dedecek, V. Murugesan, M. Hartmann, Chem. Mater. 14 (2002) 2433.
[37] (a) S.S. Bhoware, S. Shylesh, K.R. Kamble, A.P. Singh, J. Mol. Cat. A 255 (2006) 123;
(b) S. Suvanto, J. Hukkamaki, T.T. Pakkanen, T.A. Pakkanen, Langmuir 16 (2000) 4109.
[38] E.P. Barrette, L.G. Joyner, P.P. Halenda, J. Am. Chem. Soc. 73 (1951) 373.
[39] S. Bruanaur, L.S. Deming, W.S. Deming, E.J. Teller, Am. Chem. Soc. 62 (1940) 1723.
[40] (a) X.J. Chen, Q. Li, R. Xu, F. Xiao, Angew. Chem. Int. Ed. Engl. 34 (1995) 2694;
(b) A. Jentys, N.H. Pham, H. Vinek, J. Chem. Soc., Faraday. Trans. 92 (1996) 3287;
(c) C. Zhang, W. Zhou, S. Liu, J. Phys. Chem. B 109 (2005) 24319.
[41] C. Montes, M.E. Davis, B. Murray, M. Narayana, J. Phys. Chem. 94 (1990) 6425.
[42] F.A. Cotton, G. Wilkinson, Advanced Inorganic Chemistry, Wiley, New York, 1980.
[43] A.A. Verberckmoes, M.G. Uytterhoeven, R.A. Schoonheydt, Micropor. Mesopor. Mater. 22 (1998) 165.
[44] A.A. Verberckmoes, M.G. Uytterhoeven, R.A. Schoonheydt, Zeolites 19 (1997) 180.

[45] J. Dedecek, D. Kaucy, B. Wichterlova, Micropor. Mesopor. Mater. 483 (2000) 35.
[46] J. Dedecek, B. Wichterlova, J. Phys. Chem. B 103 (1999) 1462.
[47] L. Guszi, D. Bazin, Appl. Catal. A 188 (1999) 163.
[48] G. Fierro, M.A. Eberrhardt, M. Houlla, D.M. Herculles, W.K. Hall, J. Phys. Chem. 100 (1996) 8468.
[49] P.S. Singh, K. Kosuge, V. Ramaswamy, B.S. Rao, Appl. Catal. A: Gene. 177 (1999) 149.
[50] J.M. Thomas, R. Raja, J. Organo. Chem. 689 (2004) 4110.
[51] I. L. Finar, Organic Chemistry, vol. 1, 6th edition, 617.
[52] J.D. Chen, R.A. Sheldon, J. Catal. 154 (1995) 1.
[53] S.H. Jhung, Y.S. Uh, H. Chan, Appl. Catal. 62 (1990) 61.